

# Lumino-magnetic coreshell nanoparticles as magnetic-biolabels in nanomedicine and cell therapy

Rodrigo Alberto Osorio Arciniega

<sup>1</sup>Centro de Investigación Científica y de

Educación Superior de Ensenada (CICESE), Biomedics (Cancer and Bone Research), Mexico. <sup>2</sup>Centro de Nanociencias y Nanotecnología CNyN-

UNAM, BioNanoscience

Mexico City, Mexico

[rosorioarci@gmail.com](mailto:rosorioarci@gmail.com)

**Abstract—** Ongoing approaches in nanotechnology have led to the progress of the new field of nanomedicine, which comprise many applications of nanodevices and nanomaterials for diagnostic in early stages and therapeutic aims.

More over, organic dyes and fluorescent proteins are commonly used as imaging probes in microscopy because of their small size and compatibility with biological samples. However, for long-term tracking are precarious due to their low resolution imaging and low photostability.

The key behaviour of fluorescent nanoparticles is to provide biocompatible fluorescent contrast required to visualize specific structures in cells and tissues; without such contrast a biological specimen appears largely featureless and practically impossible to analyze. Lanthanide-based luminescent nanoparticles (LNP) overture enhanced signal-to-noise ratios in the time-gated and ‘anti Stokes’ imaging modalities.

In the other hand, another biomedical tool with applications in diagnostics and therapeutics is the use of magnetic nanoparticles (MNP) *per se*. Mostly, the use of MNP has been widely studied in magnetic data recording devices, in sensors, in catalytic reactions and in various biomedical applications encompassing tissue imaging for diagnosis, drug delivery and therapeutic management of diseases. Single core-shell structure has been proposed to deliver anticancer drugs at specific locations in the body accurately, enhancing advanced diagnosis and treatment of a wide variety of cancers.

In this work we explore the characteristics of synthesis and surface modifications procedures by the design of LNP jointly with MNP. We also introduce an approach of its application as a biomarker and as hyperthermia treatment.

**Keywords—** luminescent, nanoparticles, biocompatible

## I. INTRODUCTION

Increased development of different technologies in nano scale has brought tremendous attention of materials with diverse properties. Successful exploration of biological and medical applications of nanomaterials includes biosensing, cellular imaging, bio-separation, clinical diagnosis, medical therapy, and drug delivery.

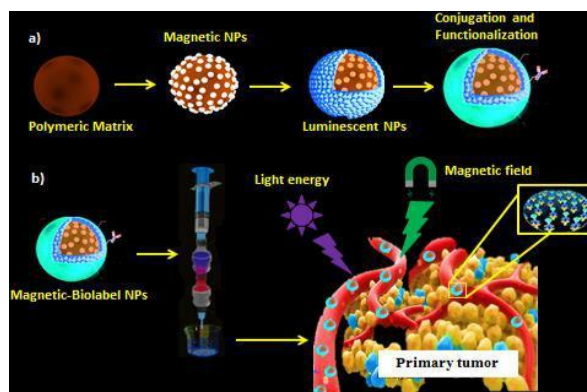
The human body has over 200 different cell lines and thousands of cell lines in the adult human body. Since the past decade, targeting different cell lines with nanomaterials has provided different techniques to overcome mainly chronic diseases. For tracking nanomaterials in live cells,

electron microscopy, surface plasmon resonance, and magnetic resonance imaging have proven to be extraordinarily useful, while these methods are time-consuming or not widely applicable to numerous types of nanomaterials with remarkable diversity.

Fluorescence techniques, (confocal optical microscopy and flow cytometry), are frequently used in biology and provide main insights into cell-nanomaterials interactions with high sensitivity. With these techniques, we can visualize molecular interactions inside cells, high time (nanosecond) resolution to trace movement of the nanomaterials inside cells, and high spatial resolution to analyze individual cells.

Conjugated polymers can provide stability and accuracy to nanoparticles. Their fluorescence is high-efficiently with a quantum yield as high as 50–90%. It has driven interest in high-sensitive and rapid-response fluorescence sensors for polynucleotides (DNA or RNA), proteins or peptides (enzymes or antibodies) and cell attachment.

In this report, we describe dual-color fluorescence labeling of magnetic nanoparticles (MP) through sol-gel method and co-precipitation synthesis. Alternatively, we describe a possible conjugation and functionalization of the magnetic-biolabels.



Scheme 1: a) Magnetic nanoparticles (MP) conjugated in a polymeric matrix with luminescent nanoparticles (LNP). b) Nanoparticles internalized in cancer cells.

### A. Luminescent Nanoparticles Synthesis

Yttrium (III) nitrate hexahydrate ( $Y(NO_3)_3 \cdot 6H_2O$ ,  $\geq 99.8\%$ ), aluminum nitrate nonahydrate ( $Al(NO_3)_3 \cdot 9H_2O$   $\geq$

99.9%), europium (III) nitrate hexahydrate ( $Ce(NO_3)_3 \cdot 6H_2O, \geq 99.9\%$ ), tartaric acid  $C_4H_6O_6$ .

$Y_3Al_5O_{12}:Eu^{3+}$  nanoparticles were synthesized by sol gel method as previously reported. Optimal stoichiometric quantity of the metal precursors was analyzed. Herein, tartaric acid was used as chelating agent in a proportion of 1:3. To mix the precursors materials, 40mL of deionized water was added under rigorous magnetic stirring for 24h at room temperature, until obtained a transparent solution.

Subsequently, we proceeded to heat at  $80^\circ C$  in order to evaporate the excess of water and accelerate the polyesterification reaction.

The solids were collected and milled with a pestle and mortar. Finally, the powder was annealed at  $1100^\circ C$  for 3h, in order to obtain an orange  $Y_3Al_5O_{12}:Eu^{3+}$  nanocrystalline powder.

### B. Magnetic Nanoparticles Synthesis

To obtain homogeneous magnetite nanoparticles, the following reactions.  $2Fe^{3+} + Fe^{2+} + 8OH^- \rightarrow Fe_3O_4 \downarrow + 4H_2O \uparrow$  The synthesis of magnetite nanoparticles ( $Fe_3O_4$ ) was carried out in aqueous solution without any surfactant. A stoichiometric combination of  $Fe^{3+} / Fe^{2+}$  in relation 2: 1 of iron chloride and ferrous chloride in a basic medium by means of pH preparation = 11-12 In addition, 0.85 mL of 12.1 N HCl and 25 mL of water purified, deoxygenated water was added.

The magnetic nanoparticles used in this study were colloidal iron oxide prepared by co-precipitation of ferrous and ferric salts in ammonia solution.

The colloidal nanoparticles had negative surface charges and hydrodynamic size in the range from 30–50 nm in aqueous solution.

## II. RESULTS

$Y_3Al_5O_{12}:Eu^{3+}$  NPs were produced using sol gel method, and an after treatment procedure of post annealed at  $1100^\circ C$ . Scheme 1 shows how nanoparticles can be produce and its corresponding application in an *in vivo* analysis. XRD pattern of  $Y_3Al_5O_{12}:Eu^{3+}$  NPs was in concordance with JCODS-03-065-3181, indicating the presence of a cubic crystal phase of YAG matrix (Fig. 1). Presence of an intense sharp peak indices (222) suggested the presence of crystalline structure. Moreover, Scherrer analysis indicated a crystallite size average of  $50.87 \pm 5nm$ .

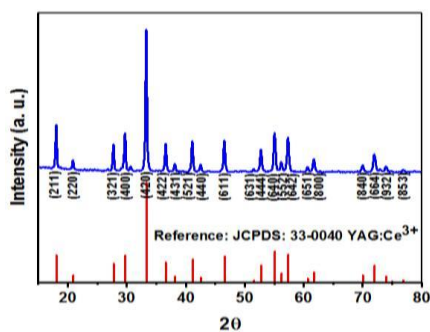


Fig. 1: X Ray diffraction pattern of  $Y_3Al_5O_{12}:Eu^{3+}$  NPs .

TEM analysis indicated the presence of agglomerates, due to the presence of van der Waals forces between the nanoparticles and an average size of  $50 \pm 5nm$ .

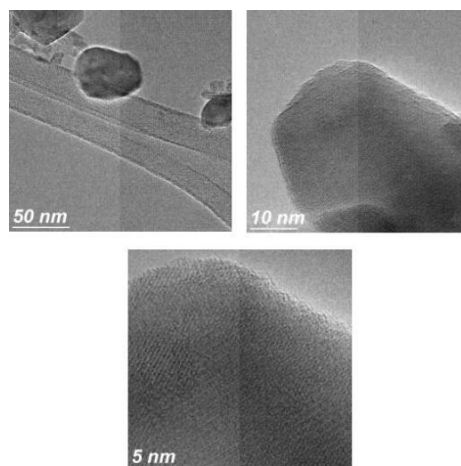


Fig. 2: TEM images of  $Y_3Al_5O_{12}:Eu^{3+}$  NPs a) 50nm, b) 10nm, c) 5nm.

Photoluminescence properties were characterized by the excitation/emission analysis were  $\lambda_{exc}:250$  and  $\lambda_{exc}:590$ . At these europium concentrations the distance between  $Eu^{3+}$  ions becomes smaller causing resonant energy transfer thus sending excitation energy to the quenching center (Fig. 3).

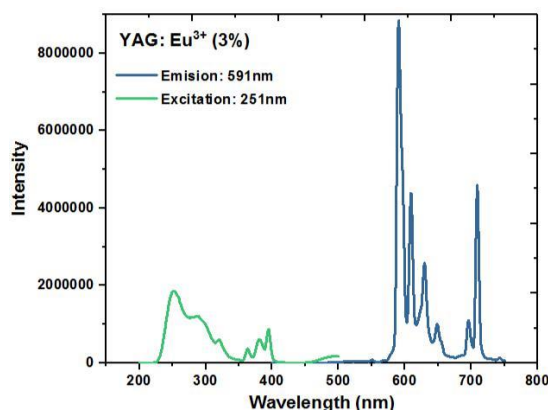
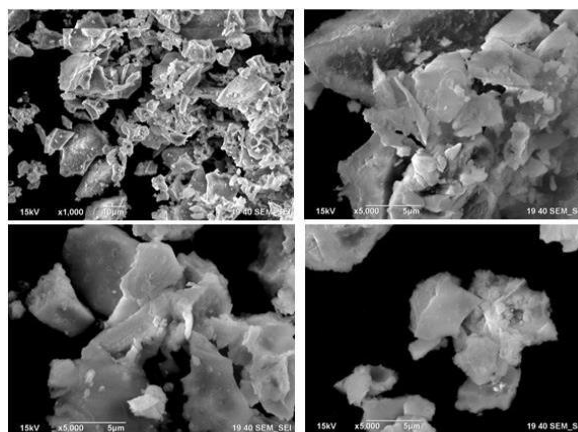


Figure 3: Photoluminescence properties of  $Y_3Al_5O_{12}:Eu^{3+}$  NPs excitation and emission spectra.

Moreover, SEM analysis showed a defined bulk structure of the  $Y_3Al_5O_{12}:Eu^{3+}$  NPs, were we confirmed the morphology of the crystalline. We noticed agglomerations and confinement by AFM analysis (Fig. 4).



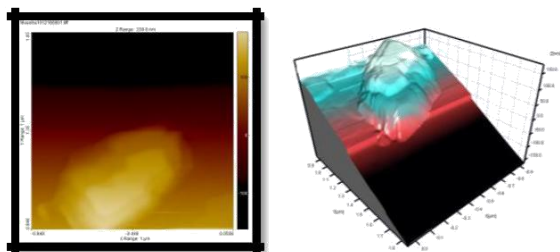


Figure 4: AFM and SEM analysis, 10µm and 5µm.

To confirm that our samples had the elements we required during the sol gel synthesis, we performed an Energy dispersive X-Ray spectrometer (EDS) analysis. We obtained the elements that corresponded to (C) Carbon, due to the SEM tape (O) Oxygen, (Al) aluminum and (Y) yttrium (Fig. 5).

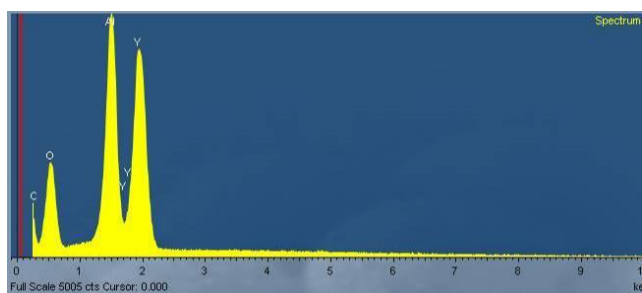


Figure 5: EDS analysis, different elements (C),(Al),(Y) and (O).

To confer magnetic properties to the luminescent nanoparticles we decided to synthesis Magnetic Nps by coprecipitation method. We developed Magnetite Nps by adding Fe(II) and Fe (III). Afterwards, we developed TEM analysis to confirm the structure, morphology and size of the magnetic nanoparticles. Results showed a nanoparticle size of  $8\pm 2\text{nm}$  (Fig. 6).

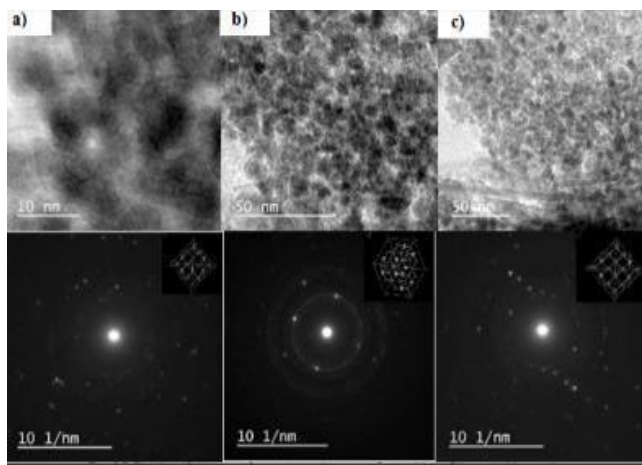


Figure 6: TEM analysis at different magnifications 10nm and 50nm.

We decided to combine the  $\text{Y}_3\text{Al}_5\text{O}_{12}:\text{Eu}^{3+}$  NPs and Magnetite NPs in a polymer matrix made of PVA by centrifugation, and with different concentrations to conjugate our nanoparticles. TEM images showed polydispersity of the matrix and the magnetic and luminescent nanoparticles attached to the matrix (Fig. 7).

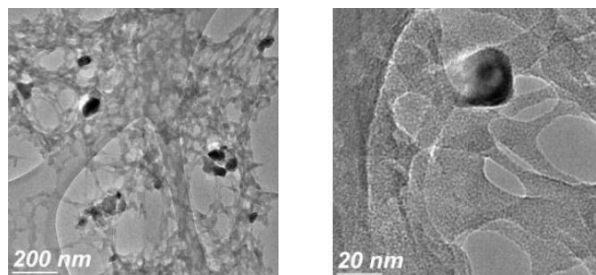


Figure 7: TEM micrographs 200 nm and 20 nm PVA polymer + Magnetic NPs + Luminescent Nanoparticles.

To verify that the nanoparticles could catchment a cell line, we performed a internalization assay. We administrated a dosis of  $1\mu\text{g}$  of the luminomagnetic NPs + the polymer to the cell line MDA-293 (breast cancer cell line) and with a neodymium magnet, we were able to direct the NPs to the cells. Moreover we demonstrated that the NPs can internalized by endocytosis method. Finally, by Confocal microscopy we noticed the capitation of the NPs (Fig.8).

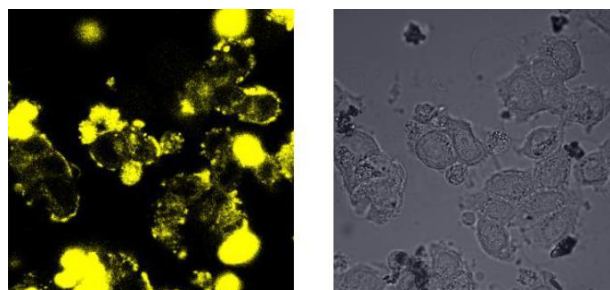


Figure 8: CM micrographs were PVA polymer + Magnetic NPs + Luminescent Nanoparticles internalized breast cancer cell line.

### III. CONCLUSION

In summary, we synthesized luminescent-magnetic nanoparticles in a polymer matrix with low toxicity that can be used as a fluorescent magnetic detection method for cancer *in vivo*. This work ensures evidence that justify future research in the cancer treatment and diagnosis field. In combination with actual detection methods, it would be possible to achieve high resolution in real time providing the detection of deeply precise located tumors.

### REFERENCES

- [1] G. Eason, B. Noble, and I. N. Sneddon, "On certain integrals of Lipschitz-Hankel type involving products of Bessel functions," *Phil. Trans. Roy. Soc. London*, vol. A247, pp. 529–551, April 1955. (*references*)
- [2] J. Clerk Maxwell, *A Treatise on Electricity and Magnetism*, 3rd ed., vol. 2. Oxford: Clarendon, 1892, pp.68–73.

- [3] I. S. Jacobs and C. P. Bean, "Fine particles, thin films and exchange anisotropy," in *Magnetism*, vol. III, G. T. Rado and H. Suhl, Eds. New York: Academic, 1963, pp. 271–350.
- [4] K. Elissa, "Title of paper if known," unpublished.
- [5] R. Nicole, "Title of paper with only first word capitalized," *J. Name Stand. Abbrev.*, in press.
- [6] Y. Yorozu, M. Hirano, K. Oka, and Y. Tagawa, "Electron spectroscopy studies on magneto-optical media and plastic substrate interface," *IEEE Transl. J. Magn. Japan*, vol. 2, pp. 740–741, August 1987 [Digests 9th Annual Conf. Magnetism Japan, p. 301, 1982].
- [7] M. Young, *The Technical Writer's Handbook*. Mill Valley, CA: University Science, 1989.